Contemporary Mathematics
https://ojs.wiserpub.com/index.php/CM/

Research Article

Fractal Analysis via Extended Fibonacci-Mann Iteration

Zaib Un Nisa[1], Tayyab Kamran[1,2], Umar Ishtiaq[3], Ioan-Lucian Popa[4,5], Mohammad Akram[6*]

[1] Department of Mathematics, Quaid-i-Azam University, Islamabad, 45320, Pakistan
[2] Center for Theoretical Physics, Khazar University, 41 Mehseti Str., Baku, AZ1096, Azerbaijan
[3] Office of Research, Innovation and Commercialization, University of Management and Technology, Lahore, 54770, Pakistan
[4] Department of Computing, Mathematics, and Electronics, "1 Decembrie 1918" University of Alba Iulia, 510009, Alba Iulia
[5] Faculty of Mathematics and Computer Science, Transilvania University of Brasov, Iuliu Maniu Street 50, Brasov, 500091, Romania
[6] Department of Mathematics, Faculty of Science, Islamic University of Madinah, Madinah, 42351, Saudi Arabia
E-mail: akram@iu.edu.sa

Received: 1 August 2025; **Revised:** 14 October 2025; **Accepted:** 15 October 2025

Abstract: In this paper, we propose an extended iteration of the generalized Fibonacci-Mann technique to establish an escape condition for functions of the form $\sin(\zeta^n) + a\zeta + c$, where a and c are complex constants, $n \geq 2$, and ζ is a complex variable. Using an s-convex combination framework, the proposed approach refines existing procedures and enables the generation of novel Mandelbrot and Julia sets. Furthermore, we provide numerical examples and graphic demonstrations to illustrate the efficiency of this novel technique.

***Keywords*:** fixed point, convergence, iterative schemes, fractals

MSC: 39B12, 37F10

1. Introduction

Fractals are intricate geometric structures characterized by self-similarity and complexity at various scales, making them a significant area of study in mathematics. Numerous studies in the pure and applied sciences have been encouraged by their recursive patterns, which display detail at arbitrarily small magnifications. The study of fractals has become the most intriguing field of study because of self-similarity [1, 2]. The study of fractals began at the turn of the 20th century when French mathematician Gaston Maurice Julia and French astronomer and mathematician Pierre Joseph Louis Fatou separately examined the behavior of iterated complex functions. The consecutive approximations of the complex function $f(\zeta) = \zeta^2 + c$, where c is a complex number and ζ is a complex variable, were discovered through their investigation of complex dynamics. Mandelbrot transformed the field in the 1970s by first using the term fractal geometry and drawing the now-famous Mandelbrot set, thus focusing on the deep and intriguing structure of such repeating processes [3].

In recent years, a considerable number of researchers have modified classical fractal sets such as Julia and Mandelbrot using different iterative methods. For instance, Rani and Kumar [4] were among the first to introduce the concept of superior sets by applying the Mann iteration scheme. Subsequently, Chauhan et al. [5] advanced this direction by employing the Ishikawa iteration to generate relative superior Julia sets. The S-iteration process was later used in multiple studies [6, 7] to construct fractal variants such as tricorns and multicorns, further diversifying the geometric output of iterative fractals.

Copyright ©2026 Mohammad Akram, et al.
DOI: https://doi.org/10.37256/cm.7220268103
This is an open-access article distributed under a CC BY license
(Creative Commons Attribution 4.0 International License)
https://creativecommons.org/licenses/by/4.0/

Another interesting development came from Rani and Chugh [8], who utilized the three-step Noor iteration to form new Julia and Mandelbrot structures. Many of these iterative strategies have been examined alongside s-convex combinations, which enhance the convergence behavior and alter the resulting geometry [9–12].

Fractals are not only mathematical constructs but also have practical relevance in several fields. In chaotic dynamics, fractal structures appear in complex system modeling and neural networks [13, 14]. In physical and biological systems, fractals are also pervasive. A classic example is a fern, where each branch resembles both the overall structure and its smaller sub-branches. Similar patterns are observed in coastlines, terrains, trees, river networks, blood vessels, and other natural systems. These intricate structures can often be explained by the repeated application of simple rules, known as fractal codes. Fractal shapes exist throughout the human body, in lungs, blood vessels, and neurons. Fractals can also be used to aid diagnosis of abnormal heart rhythms and tumours [15]. Fractals are widely used in computer graphics and visual effects, where they provide a powerful tool for creating highly detailed and realistic images. They are employed to generate textures and landscapes in video games, movies, and virtual environments, producing results that appear extremely lifelike. In addition, fractals play an important role in image generation, geometric modeling, and texture synthesis, where their self-similar structures allow complex scenes to be represented through relatively simple iterative rules [16].

Fractals generated through fixed-point iteration methods also serve practical purposes in simulating natural phenomena, such as the geometry of coastlines or the branching of plants. These structures are integral to high-resolution graphical modeling and are used to test parallel computing algorithms and address large-scale computational challenges [17, 18]. Recent interdisciplinary applications, such as those in supply chain dynamics, further illustrate the interdisciplinary value of fractal-based methods. Julia sets, for example, have been employed to analyze the connectivity of attraction basins in dual-channel supply chains, providing insights into stability and robustness in pricing strategies. By identifying the influence of initial conditions and parameters on system stability, fractal methods aid in designing effective interventions to prevent instability caused by factors like excessive online preferences [19]. Additionally, the connectivity of Julia sets offers a framework for evaluating system robustness under varying conditions, guiding decision-making in real-world markets. These connectivity measures have informed control strategies to restore market stability, demonstrating how fractal analyses bridge mathematical theory with actionable insights in complex, multi-variable systems.

Other extensions have considered the Jungck-Mann and Jungck-Ishikawa schemes in the presence of s-convexity, as noted by Antal et al. [20]. Further visualization of complex fractals using Noor and S-iteration schemes with s-convexity was addressed in [21], suggesting a strong correlation between iterative design and the complexity of the generated geometry.

A recent development in fractal generation is the Fibonacci-Mann iteration. This method extends the traditional Mann process by using the Fibonacci sequence to add a kind of memory to the steps. Instead of relying only on the last value, it also considers earlier values in the sequence [22, 23].

Section 2 explains crucial definitions and ideas that are required for the study. In Section 3, we investigate an extended version of the generalized Fibonacci-Mann iteration escape requirement for the complex function in the complex plane using s-convex combinations. Section 4 presents generalizations and variations of the classical Julia and Mandelbrot sets using modified iterative schemes. We examine numerical instances in Section 5, and Section 7 concludes our study.

2. Preliminaries

This section presents definitions and notations for the readers' comprehension. Let $\mathbb{C}$ represent the set of complex numbers, $\mathbb{R}$ signify the set of real numbers, and $\mathbb{N}$ designate the set of positive integers. The subsequent section delineates the definitions of the Julia and Mandelbrot sets, two significant fractal structures. These sets are crucial to the research conducted for this study.

Definition 1 [24] For a function $\mathscr{P} : \mathbb{C} \to \mathbb{C}$, the filled Julia set $E_{\mathscr{P}}$ consists of the set of points in the complex plane whose orbits under $\mathscr{P}$ are limited

$$E_{\mathscr{P}} = \{u \in \mathbb{C} : \{|\mathscr{P}_m(u)|\}_{m=0}^{\infty} \text{ is bounded}\}, \tag{1}$$

and the m-th iteration of the function $\mathscr{P}_r$ is indicated by $\mathscr{P}_r^m$. The filled Julia set $\mathscr{P}_{u_r}$ is bounded by the Julia set $J_{\mathscr{P}_r}$ of $\mathscr{P}_r$.

Definition 2 [25] Let a function $\mathscr{P}_u : \mathbb{C} \to \mathbb{C}$ and $u \in \mathbb{C}$ be a parameter. The Mandelbrot set S is the set of all points $u \in \mathbb{C}$ for which the filled Julia set $E_{\mathscr{P}_u}$ is connected

$$S = \{u \in \mathbb{C} : E_{\mathscr{P}_u} \text{ is connected}\}, \tag{2}$$

and equivalently $S_{\mathscr{P}_u}$ can be defined as

$$S = \{u \in \mathbb{C} : \{|\mathscr{P}_u^m(\vartheta)|\} \nrightarrow \infty \text{ as } m \to \infty\},$$

where ϑ represents any critical point of $\mathscr{P}_u$.

We then go over a variety of iterative techniques, which are crucial resources for the research described in this work. Since this is adequate for our research goals, we shall define iterative methods in the context of $\mathbb{C}$, even if many of them are first developed in normed or abstract spaces.

Definition 3 [26] For a complex-valued self-mapping $\mathscr{P} : \mathbb{C} \to \mathbb{C}$ we define the Mann iteration scheme $\{u_g\}$ as follows:

$$\begin{cases} u_0 \in \mathbb{C} \\ \\ u_{g+1} = (1 - \phi_g)\, u_g + \phi_g \mathscr{P} u_g. \end{cases} \tag{3}$$

for all $g \in \mathbb{N} \cup \{0\}$, where $\phi_g \in [0,\ 1]$ for all $g \in \mathbb{N} \cup \{0\}$.

This paper's inspiration comes from the subsequent iteration, which is as follows:

Definition 4 [27] Let $s \in (0,\ 1]$ and consider a sequence consisting of $u_1,\ u_2,\ u_3,\ \ldots,\ u_n \in \mathbb{C}$, then the s-convex combination is defined as:

$$\beta_1^s \cdot u_1 + \beta_2^s \cdot u_2 + \beta_3^s \cdot u_3 + \cdots + \beta_n^s \cdot u_n, \tag{4}$$

where $\beta_g \geq 0$ and $\sum_{g=1}^{n} \beta_g = 1$.

Definition 5 [28] For a self-mapping $\mathscr{P} : \mathbb{C} \to \mathbb{C}$, the iteration scheme $\{v_g\}$ of Noor iteration is defined as:

$$\begin{cases} u_0 \in \mathbb{C} \\ w_g = (1-\psi_g)v_g + \psi_g \mathscr{P} v_g \\ z_g = (1-\mu_g)v_g + \mu_g \mathscr{P} w_g \\ u_{g+1} = \mathscr{P} z_g, \end{cases} \tag{5}$$

for all non-negative integers $g \in \mathbb{N} \cup \{0\}$, where each $\psi_g,\ \mu_g \in [0,\ 1]$.

Significant progress in iterative techniques was made in 2021, especially with the creation of an innovative approach that adds the idea of s-convexity to the Mann and Picard-Mann iterations. This iteration's consequence is as follows:

Definition 6 [29] For a self-map $\mathscr{P} : \mathbb{C} \to \mathbb{C}$ with $s \in (0,\ 1]$, and with the s convexity, Iteration scheme $\{u_g\}$ of Mann is as follows:

$$\begin{cases} u_0 \in \mathbb{C} \\ u_{g+1} = (1-\phi_g)^s u_g + \phi_g^s \mathscr{P} u_g, \end{cases} \tag{6}$$

for all $g \in \mathbb{N} \cup \{0\}$, where $\phi_g \in [0,\ 1]$ for all $g \in \mathbb{N} \cup \{0\}$.

Definition 7 [29] For a self-mapping $\mathscr{P} : \mathbb{C} \to \mathbb{C}$ with $s \in (0,\ 1]$, the iteration scheme $\{u_g\}$ of Picard-Mann with s-convexity as follows:

$$\begin{cases} u_0 \in \mathbb{C} \\ v_g = (1-\phi_g)^s u_g + \phi_g^s \mathscr{P} u_g \\ u_{g+1} = \mathscr{P} v_g, \end{cases} \tag{7}$$

for all non-negative integers $g \in \mathbb{N} \cup \{0\}$, where each is constrained to $\phi_g \in [0,\ 1]$.

Definition 8 [23] Consider the map $\mathscr{P} : \mathbb{C} \to \mathbb{C}$, with initial point $\zeta_0 \in \mathbb{C}$. Assume the parameters $\phi_m \in [0,\ 1]$ and $m \in \mathbb{N}$. Also $0 < s \leq 1$. Assume that $\tau = \inf\{\phi_m\} > 0$. We present the generalized Fibonacci-Mann iteration incorporating s-convexity as:

$$\zeta_m = \phi_m^s \mathscr{P}^{h(m)}(\zeta_m) + (1-\phi_m)^s \zeta_m.$$

3. An escape criteria via extended generalized Fibonacci-Mann iteration process

Consider that

$$\left| 1 - \frac{\zeta^{2n}}{3!} + \frac{\zeta^{4n}}{5!} \ldots \right| \geq |\mu_1|,$$

unless $|\mu_1| = 0$ for those values of ζ, where $|\mu_1| \in (0,\ 1]$. After that, we've

$$|\sin(\zeta^n)| = \left|\zeta^n - \frac{\zeta^{3n}}{3!} + \frac{\zeta^{5n}}{5!} - \ldots\right| = |\zeta^n|\left|1 - \frac{\zeta^{2n}}{3!} + \frac{\zeta^{4n}}{5!} - \ldots\right|.$$

As a result,

$$|\sin(\zeta^n)| \geq |\zeta^n|\,|\mu_1|, \tag{8}$$

where μ_1 and $\zeta \in \mathbb{C}$.

Definition 9 Consider the complex-valued mapping $\mathscr{P} : \mathbb{C} \to \mathbb{C}$, with $\zeta_0 \in \mathbb{C}$ and parameters $\phi_m \in [0,\ 1]$ and $m \in \mathbb{N}$. Also $0 < s \leq 1$. Assume $\tau = \inf\{\phi_m\} > 0$. An extended version of the generalized Fibonacci-Mann iteration that includes s-convexity is outlined below

$$\begin{cases} v_m = \phi_m^s \mathscr{P}^{h(m)}(\zeta_m) + (1-\phi_m)^s \zeta_m \\ y_m = \mathscr{P}^2 v_m \\ \zeta_{m+1} = \mathscr{P}^2 y_m, \end{cases} \tag{9}$$

$\mu_1 \in (0,\ 1]$ is the primary iteration weight, $\{\phi_m\}$ is a control sequence with $\phi = \inf\{\phi_m\} > 0$, and $s \in (0,\ 1]$ in which $h(m)$ is defined as the generalized Fibonacci number.

Theorem 1 Let $a,\ c \in \mathbb{C}$ and $n \geq 2$ be given, and consider the complex function $\mathscr{P}a,\ c(\zeta) = \sin(\zeta^n) + a\zeta + c$. Using an extended form of the generalized Fibonacci-Mann iteration that incorporates s-convexity, define a sequence $\zeta_m,\ m \in \mathbb{N}$. Suppose that

$$|\zeta| \geq |v| \geq |c| > \left(\frac{2(\mathfrak{T}|a|+1)}{s\phi|\mu_1|}\right)^{\frac{1}{n-1}}, \tag{10}$$

where $\mu_1 \in (0,\ 1]$ is the primary iteration weight, $\{\phi_m\}$ is a control sequence with $\phi = \inf\{\phi_m\} > 0$, and $s \in (0,\ 1]$. Then it follows that $|\zeta_m|$ tends to infinity as m approaches infinity.

Proof. Assume $\mathscr{P}_{a,\,c}(\zeta) = \sin(\zeta^n) + a\zeta + c$, $\zeta_0 = \zeta$ and

$$\begin{cases} v_m = \phi_m^s \mathscr{P}^{h(m)}(\zeta_m) + (1-\phi_m)^s \zeta_m \\ y_m = \mathscr{P}^2 v_m \\ \zeta_{m+1} = \mathscr{P}^2 y_m. \end{cases}$$

For $m = 0$, $h(0) = 1$. By using the binomial expansion, for $s \in (0,\ 1]$ and $0 < \phi < 1$, we have

$$(1-\phi)^s = 1 - s\phi + \frac{s(s-1)}{2!}\phi^2 - \frac{s(s-1)(s-2)}{3!}\phi^3 + \cdots.$$

Since $s-1 \leq 0$ for $s \in (0,\ 1]$, it follows that $s(s-1) \leq 0$. Hence, the quadratic term

$$\frac{s(s-1)}{2!}\phi^2 \leq 0.$$

Similarly, all higher-order coefficients beyond the linear term are also nonpositive. Therefore,

$$(1-\phi)^s \leq 1-s\phi, \quad 0<\phi<1,\ 0<s\leq 1.$$

Consider,

$$|v_0| = \left|\phi_0^s \mathscr{P}_{a,\,c}^{h(0)}(\zeta) + (1-\phi_0)^s\zeta\right| = \left|\phi_0^s\left[\sin(\zeta^n)+a\zeta+c\right] + (1-\phi_0)^s\zeta\right|.$$

Since $\phi = \inf\{\phi_m\} > 0$, we have $\phi_0 \in (0,\ 1]$ and hence $\phi_0^s \geq s\phi_0$. From these facts and the condition $|\xi| \geq |c|$, we obtain

$$\begin{aligned}
|v_0| &\geq \left|s\phi_0\left[\sin(\zeta^n)+a\zeta+c\right] + (1-\phi_0)^s\zeta\right| \\
&\geq s\phi_0\left|\sin(\zeta^n)+a\zeta+c\right| - (1-\phi_0)^s|\zeta| \\
&\geq s\phi_0|\sin(\zeta^n)| - |(1-\phi_0)^s||\zeta| - s\phi_0|a||\zeta| - s\phi_0|c|.
\end{aligned}$$

By using inequality (8), we get

$$|v_0| \geq s\phi_0|\mu_1||\zeta^n| - (1-s\phi_0)|\zeta| - s\phi_0|a||\zeta| - s\phi_0|c| \geq s\phi_0|\mu_1||\zeta^n| - |\zeta|\left((1-s\phi_0) + s\phi_0|a| + s\phi_0\frac{|c|}{|\zeta|}\right).$$

By simplifying the coefficient of $|\zeta|$, we get

$$|v_0| \geq |\zeta|(\mathfrak{T}|a|+1)\left(\frac{s\phi\,|\mu_1||\zeta^{n-1}|}{\mathfrak{T}|a|+1} - 1\right).$$

Finally, we obtain

$$|v_0| \geq \frac{|v_0|}{\mathfrak{T}|a|+1} \geq |\zeta|\left(\frac{s\phi\,|\mu_1|\,|\zeta^{n-1}|}{\mathfrak{T}|a|+1} - 1\right). \tag{11}$$

Set $\nu_1 = \mathscr{P}_{a,\,c}(v_0)$, $\nu_2 = \mathscr{P}_{a,\,c}^2(v_0)$, $\nu_3 = \mathscr{P}_{a,\,c}^3(v_0)$, and $\nu_4 = \mathscr{P}_{a,\,c}^4(v_0)$. It can be seen from inequality (10)

$$\left|v^{n-1}\right| |\mu_1| \geq |a| + 2. \tag{12}$$

Using inequalities (12) and (8), we obtain

$$\frac{|v_1|}{|v_0|} = \frac{\left|\sin\left(v_0^n\right) + av_0 + c\right|}{|v_0|} \geq \frac{\left|\sin\left(v_0^n\right)\right| - |a|\,|v_0| - |c|}{|v_0|}$$

$$\geq \frac{\left|v_0^n\right| |\mu_1| - |a|\,|v_0| - |v_0|}{|v_0|} = \left|v_0^{n-1}\right| |\mu_1| - |a| - 1 \geq 1,$$

and hence

$$|v_1| \geq |v_0|.$$

By similar reasoning, we can see that

$$|\zeta_1| = |v_4| \geq |v_0|.$$

For $m = 1$, $h(1) = 1$. Applying similar reasoning and using inequality (11), we have

$$|\zeta_2| \geq |\zeta_1| \left(\frac{s\phi\,|\mu_1|\left|\zeta_1^{n-1}\right|}{\mathfrak{T}|a| + 1} - 1\right)$$

$$\geq |\zeta| \left(\frac{s\phi\,|\mu_1|\left|\zeta^{n-1}\right|}{\mathfrak{T}|a| + 1} - 1\right) \left(\frac{s\phi\,|\mu_1|\left|\zeta_1^{n-1}\right|}{\mathfrak{T}|a| + 1} - 1\right) \tag{13}$$

$$\geq |\zeta| \left(\frac{s\phi\,|\mu_1|\left|\zeta^{n-1}\right|}{\mathfrak{T}|a| + 1} - 1\right)^2,$$

and, so

$$|\zeta_2| \geq |\zeta| \left(\frac{s\phi\,|\mu_1|\left|\zeta^{n-1}\right|}{\mathfrak{T}|a| + 1} - 1\right)^2. \tag{14}$$

Using inequality (11) along with the fact that $|\zeta| \geq |c| > \left(\frac{2(\mathfrak{T}|a| + 1)}{s\phi\,|\mu_1|}\right)^{\frac{1}{n-1}}$, we have $|\zeta_1| \geq |\zeta|$ and this implies

$$|\zeta_1|\left(\frac{s\phi\,|\mu_1|\,|\zeta_1^{n-1}|}{\mathfrak{T}|a|+1}-1\right)\geq|\zeta|\left(\frac{s\phi\,|\mu_1|\,|\zeta^{n-1}|}{\mathfrak{T}|a|+1}-1\right). \tag{15}$$

Again, using the inequalities $|\zeta_1|\geq|\zeta|\geq|c|>\left(\frac{2(\mathfrak{T}|a|+1)}{s\phi\,1}\right)^{\frac{1}{n-1}}$ and (13), we find $|\zeta_2|\geq|\zeta_1|$. By repeating this process to the l-th term, we obtain

$$|\zeta_l|\geq|\zeta|\left(\frac{s\phi\,|\mu_1|\,|\zeta^{n-1}|}{\mathfrak{T}|a|+1}-1\right)^{l}.$$

Then, because of inequality (10), we have

$$\frac{s\phi\,|\mu_1|\,|\zeta^{n-1}|}{\mathfrak{T}|a|+1}-1>1,$$

where $|\mu_1|\in(0,\ 1]$. Consequently, the orbit of ζ tends to infinity, that is, $|\zeta_k|\to\infty$ as $k\to\infty$. □

4. Generalizations and variations of Julia and Mandelbrot sets

We use MATLAB (R2022b) to investigate generalized forms of classical fractals based on the transcendental sine function $\mathscr{P}_{a,\,c}(\zeta)=\sin(\zeta^n)+a\zeta+c$, where $a,\ c\in\mathbb{C}$, $n\geq 2$, and ζ is a complex variable. Unlike the traditional quadratic case, this formulation introduces oscillatory behavior that enriches the dynamics of the generated sets.

The mathematical methods were established using MATLAB R2022b, and the experiments were carried out via a computer with a 12$^{\text{th}}$ Gen Intel® Core™ i5-1235U processor operating at 1.30 GHz, with 10 cores and 12 logical processors, and 8 GB of RAM. Each created image had a resolution of 600 × 600 pixels.

To analyze these structures, we design two algorithms. Algorithm 1 generates Julia sets by iterating initial points in the complex plane under the escape condition of $\mathscr{P}_{a,\,c}$, using the extended generalized Fibonacci-Mann iteration with s-convexity. Algorithm 2 applies the same iterative principle in the parameter space, constructing corresponding Mandelbrot sets.

For a better visual representation, a widely used standard colormap was applied to assign colors to data points, known as the "Jet" colormap. Figure 1 shows how the "jet" colormap is used to generate the Julia and Mandelbrot sets.



Figure 1. Julia and Mandelbrot sets are created by using a color map

Algorithm 1 Generating Julia set

Input: $\mathscr{P}_{a,\,c}(\zeta)=\sin(\zeta^n)+a\zeta+c$, where $a,\ c\in\mathbb{C}$ and $n\geq 2$; $\mathscr{O}\subset\mathbb{C}$ describes the area of analysis; K-upper limit for iterations; $0<\phi_n\leq 1$, $0<\mu_1\leq 1$-tuning parameters for the extended Fibonacci Mann procedure taking s-convexity; $k,\ i$-nonzero real values; colormap $[0,\ \ldots,\ C-1]$-indicates a palette with C color levels.

Output: Julia set over region $\mathscr{O}$

1: **for** $\zeta\in\mathscr{O}$ **do**

2: $\mathscr{M}_1 = \left(\frac{2(\Im(|a|)+1)}{s\phi|\mu_1|}\right)^{\frac{1}{n-1}}$
3: $\mathscr{M} = \max(|c|, \mathscr{M}_1)$
4: $m = 0$
5: $h(0) = 1$
6: $h(1) = 1$
7: **While** $m < K$ **do**
8: **if** $m > 1$ **then**
9: $h(m) = kh(m-1) + ih(m-2)$
10: **end if**
11: $v_m = \phi_m^s \mathscr{P}^{h(m)}(\zeta_m) + (1-\phi_m)^s \zeta_m$
12: $y_m = \mathscr{P}^2 v_m$
13: $\zeta_{m+1} = \mathscr{P}^2 y_m$
14: **if** $|\zeta_{m+1}| > \mathscr{M}$ **then**
15: **break**
16: **end if**
17: $m = m+1$
18: **end while**
19: $p = \left\lfloor \frac{(C-1))\,m}{K} \right\rfloor$
20: color ζ with color map $[p]$
21: **end for**

Algorithm 2 Generating Mandelbrot Set

Input: $\mathscr{P}_{a,\,c}(\zeta) = \sin(\zeta^n) + a\zeta + c$, where $a,\ c \in \mathbb{C}$ and $n \geq 2$; $\mathscr{O} \subset \mathbb{C}$ describes the area of analysis; K-upper limit for iterations; $0 < \phi_n \leq 1$, $0 < \mu_1 \leq 1$-tuning parameters for the extended Fibonacci Mann procedure taking s-convexity; $k,\ i$-nonzero real values; colormap $[0,\ \ldots,\ C-1]$-indicates a palette with C color levels.

Output: Mandelbrot set over region $\mathscr{O}$

1: **for** $c \in \mathscr{O}$ **do**
2: $\mathscr{M}_1 = \left(\frac{2(\Im(|a|)+1)}{s\,\phi_n\,|\mu_1|}\right)^{\frac{1}{n-1}}$
3: $\mathbf{M} = \max(|c|, \mathscr{M}_1)$
4: $m = 0$
5: Compute critical points of $\mathscr{P}_{a,\,c}$:
6: $\mathscr{P}'_{a,\,c}(\zeta) = n\zeta^{n-1}\cos(\zeta^n) + a = 0$
7: **for** each critical point ζ_0 **do**
8: $h(0) = 1$
9: $h(1) = 1$
10: **while** $m \leq K$ **do**
11: **if** $m > 1$ **then**
12: $h(m) = k\,h(m-1) + i\,h(m-2)$
13: **end if**
14: $v_m = \phi_m^s \mathscr{P}^{h(m)}(\zeta_m) + (1-\phi_m)^s \zeta_m$
15: $y_m = \mathscr{P}^2 v_m$
16: $\zeta_{m+1} = \mathscr{P}^2 y_m$
17: **if** $|\zeta_{m+1}| > \mathscr{M}$ **then**
18: **break**
19: **end if**
20: $m = m+1$
21: **end while**

22: $p = \left\lfloor \frac{(C-1)m}{K} \right\rfloor$
23: color c with colormap $[p]$
24: **end for**
25: **end for**

5. Applications of fractals via proposed iteration

This section consists of two subsections. In first subsection we demonstrate some graphical examples of quadratic, cubic and quadric Julia sets and in second we present some graphs of quadratic, cubic and quadric Mandelbrot sets.

5.1 *Generation of Julia sets*

This section explains how Julia sets were generated numerically and describes the methods and parameters used to create the resulting images. Julia sets are produced by iterating complex functions and examining the behavior of points in the complex plane under repeated application of these functions.

5.1.1 *Julia set of $\mathscr{P}_{a,c}(\zeta) = \sin(\zeta^n) + a\zeta + c$, varying the parameter n*

We created cubic, quartic, quintic and sextic Julia sets using the data from Table 1 via modification of the value of parameter σ. These sets exhibit visually pleasing shapes as shown in Figure 2.

Table 1. Parameters used to generate the Julia set for various values of n

S.N.	s	t	c	σ	a	n
1	0.70	0.05	0.06	0.05	0.90	3
2	0.70	0.05	0.06	0.05	0.90	4
3	0.70	0.05	0.06	0.05	0.90	5
4	0.70	0.05	0.06	0.05	0.90	6

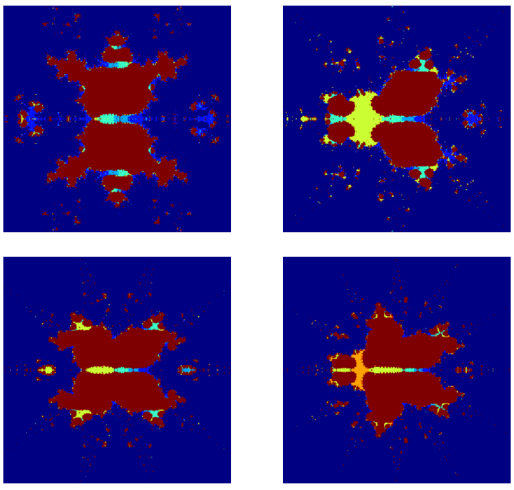


Figure 2. Effect of n on Julia set

5.1.2 *Julia set of* $\mathscr{P}_{a,\,c}(\zeta) = \sin(\zeta^n) + a\zeta + c$, *varying the parameter s*

We created visually appealing quadratic Julia sets using the data shown in Table 2 and depicted in Figure 3.

Table 2. Parameters used to generate the Julia set for various values of s

S.N.	s	t	c	σ	a	n
1	0.90	0.05	0.06	0.05	0.90	2
2	0.70	0.05	0.06	0.05	0.90	2
3	0.50	0.05	0.06	0.05	0.90	2
4	0.30	0.05	0.06	0.05	0.90	2

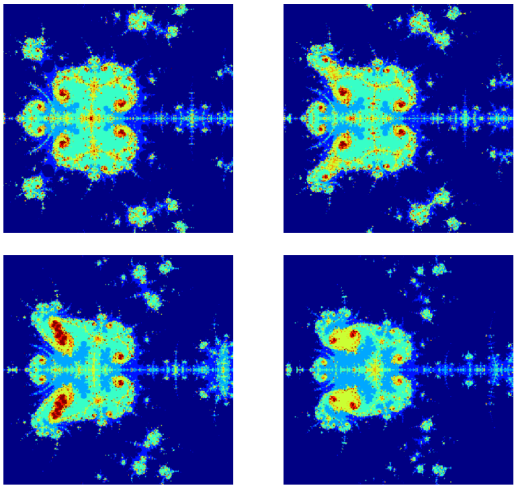


Figure 3. Effect of s on Julia set

5.1.3 *Julia set of* $\mathscr{P}_{a,\,c}(\zeta) = \sin(\zeta^n) + a\zeta + c$, *varying the parameter c*

A thorough set of parameters that produce interesting Julia sets through careful adjustments of c is shown in Table 3. Figure 4 displays these fascinating Julia sets.

Table 3. Parameters used to generate the Julia set for various values of c

S.N.	s	t	c	σ	a	n
1	0.90	0.05	0.01	0.05	0.90	2
2	0.90	0.05	0.10	0.05	0.90	2
3	0.90	0.05	−0.05	0.05	0.90	2
4	0.90	0.05	0.20	0.05	0.90	2

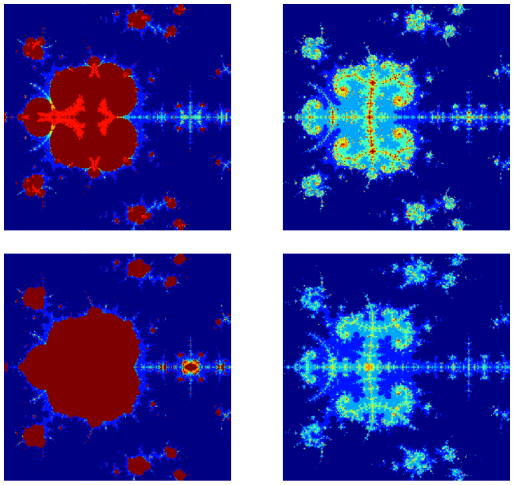


Figure 4. Effect of c on Julia set

5.1.4 *Julia set of $\mathscr{P}_{a,\,c}(\zeta) = \sin(\zeta^n) + a\zeta + c$, varying the parameter t*

Table 4 gives the list of parameters to create Julia sets by changing the parameter t, as shown in Figure 5.

Table 4. Parameters used to generate the Julia set for various values of t

S.N.	s	t	c	σ	a	n
1	0.80	0.0090	0.09	0.0100	0.90	2
2	0.80	0.1000	0.09	0.0100	0.90	2
3	0.80	0.5000	0.09	0.0100	0.90	2
4	0.80	1.0000	0.09	0.0100	0.90	2

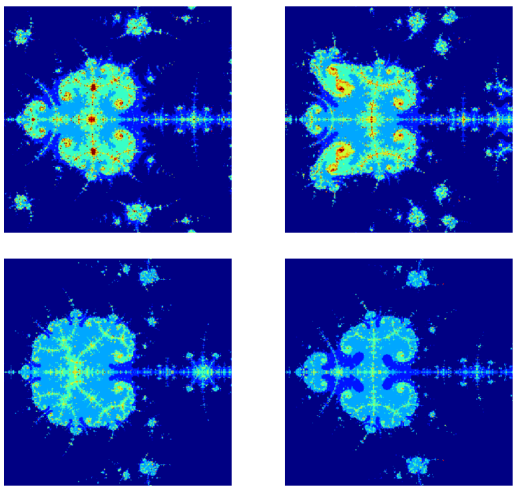


Figure 5. Effect of t on Julia set

5.1.5 *Effects of changing the parameters a to produce the Julia sets*

Table 5 gives the list of parameters to create Julia sets by changing the parameter a, as shown in Figure 6.

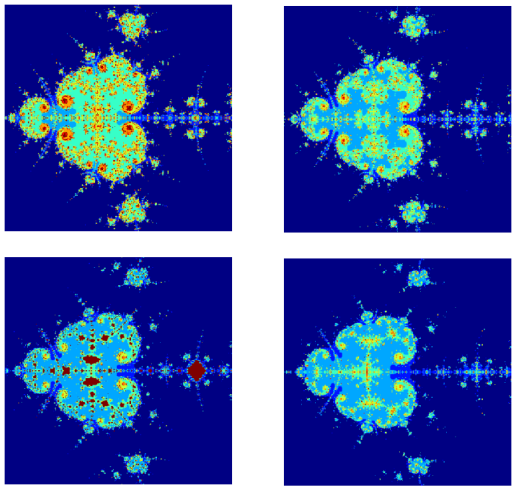


Figure 6. Effect of a on Julia set

Table 5. Parameters used to generate the Julia set for various values of a

S.N.	s	t	c	σ	a	n
1	0.90	0.90	0.07	0.10	0.60	2
2	0.90	0.90	0.07	0.10	0.70	2
3	0.90	0.90	0.07	0.10	0.80	2
4	0.90	0.90	0.07	0.10	0.90	2

5.2 *Generation of Mandelbrot sets*

This section explains how the Mandelbrot set was generated numerically. The images were created by applying an iterative algorithm with selected parameters, as summarized in the tables. The resulting figures illustrate the characteristic structure of the Mandelbrot set for the chosen ranges.

5.2.1 *Mandelbrot set of $\mathscr{P}_{a,\,c}(\zeta) = \sin(\zeta^n) + a\zeta + c$, varying the parameter n*

By altering n while maintaining the other values constant, the stunning Mandelbrot sets were produced. Table 6 lists the precise values used, and Figure 7 displays the graphics illustrating how the sets alter with various n values.

Table 6. Parameters used to generate the Mandelbrot set for various values of n

S.N.	s	t	σ	a	n
1	0.90	0.50	0.050	0.90	2
2	0.90	0.50	0.050	0.90	3
3	0.90	0.50	0.050	0.90	4
4	0.90	0.50	0.050	0.90	5

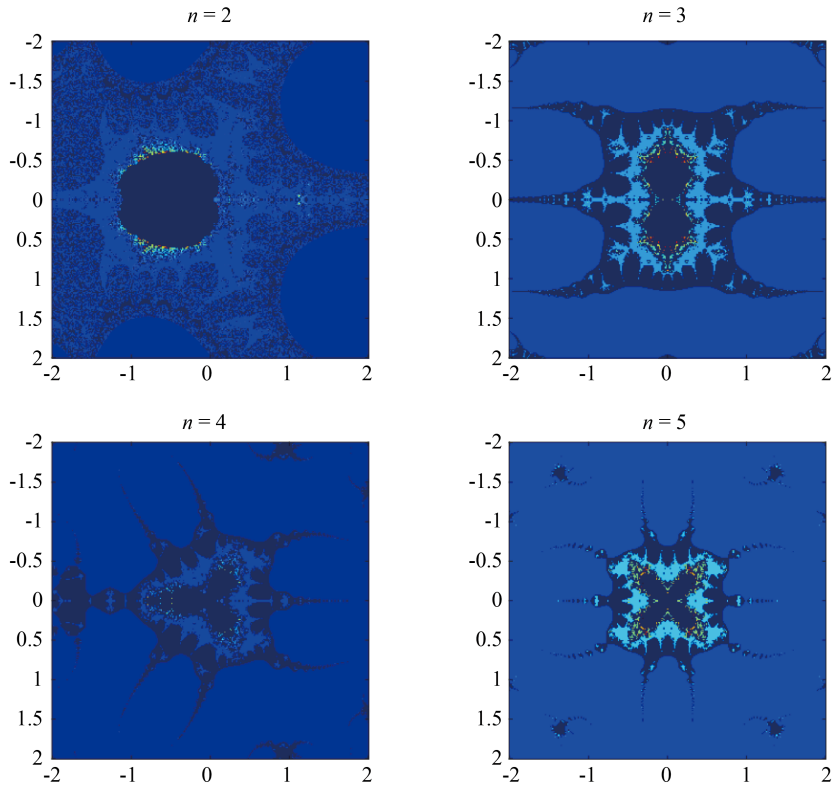
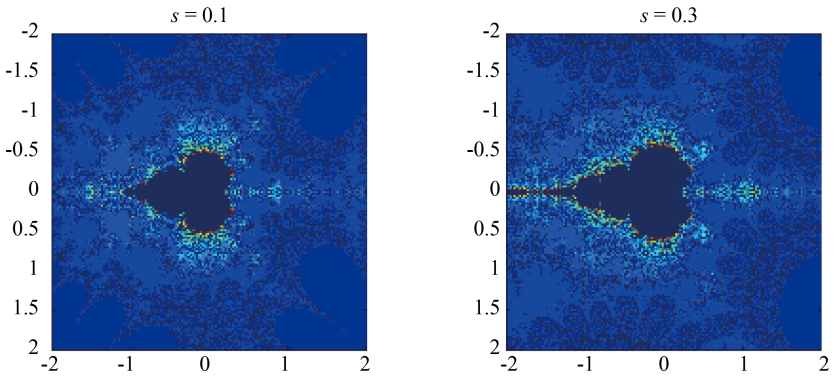


Figure 7. Effect of n on Mandelbrot set

5.2.2 *Mandelbrot set of $\mathscr{P}_{a,c}(\zeta) = \sin(\zeta^n) + a\zeta + c$, varying the parameter s*

By changing the value of s, which is the convexity parameter, while maintaining the value of other parameters constant, the visually appealing Mandelbrot sets were produced. Table 7 provides the results corresponding to different values of s, and Figure 8 shows the results graphically. The symmetry of the Mandelbrot sets is independent on s.



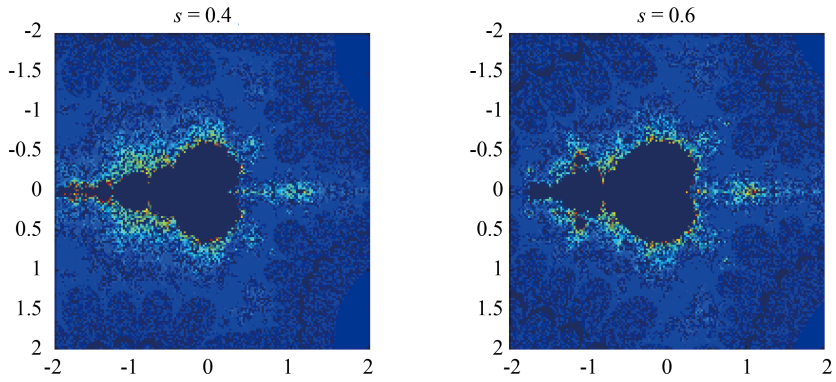


Figure 8. Effect of s on Mandelbrot set

Table 7. Parameters used to generate the Mandelbrot set for various values of s

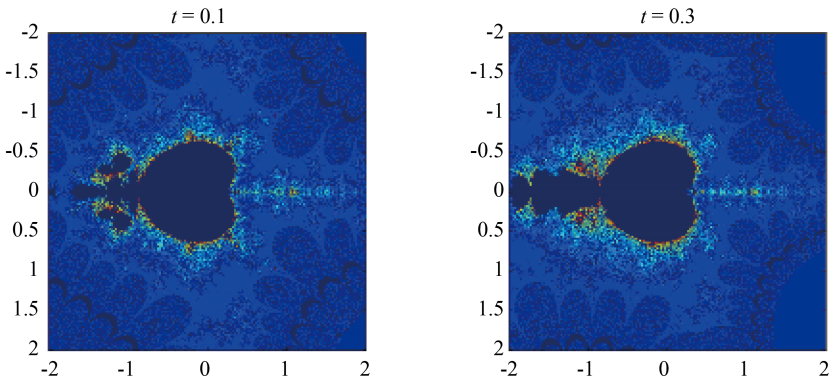
S.N.	s	t	σ	a	n
1	0.40	0.09	0.05	0.05	2
2	0.10	0.09	0.05	0.05	2
3	0.30	0.09	0.05	0.05	2
4	0.60	0.09	0.05	0.05	2

5.2.3 *Mandelbrot set of* $\mathscr{P}_{a,c}(\zeta) = \sin(\zeta^n) + a\zeta + c$, *varying the parameter t*

Thorough set of parameters that produce interesting Mandelbrot sets by adjusting the value of parameter ϕ is shown in Table 4. Figure 9 displays these eye-catching Julia sets for different values of t as provided in Table 8.

Table 8. Parameters used to generate the Mandelbrot set for various values of t

S.N.	s	t	σ	a	n
1	0.80	0.10	0.05	0.10	2
2	0.80	0.30	0.05	0.10	2
3	0.80	0.50	0.05	0.10	2
4	0.80	1.00	0.05	0.10	2



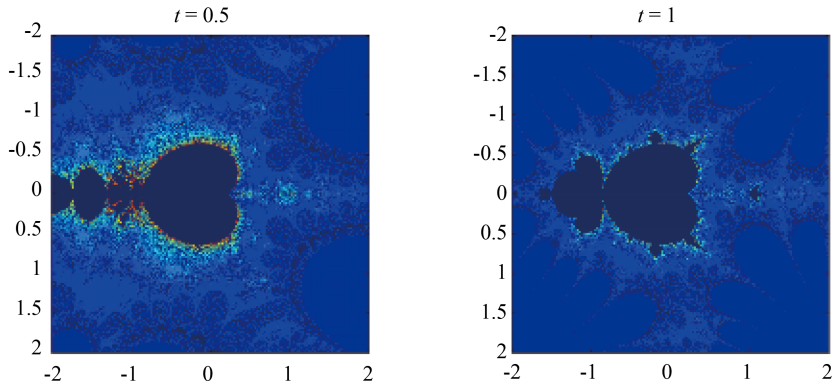


Figure 9. Effect of t on Mandelbrot set

5.2.4 *Mandelbrot set of* $\mathcal{P}_{a,c}(\zeta) = \sin(\zeta^n) + a\zeta + c$, *varying the parameter a*

While maintaining the other values of parameters constant, the visually appealing Mandelbrot sets were given by adjusting the value of ξ. The findings for various values of ξ are compiled in Table 9, and these results are shown graphically in Figure 10.

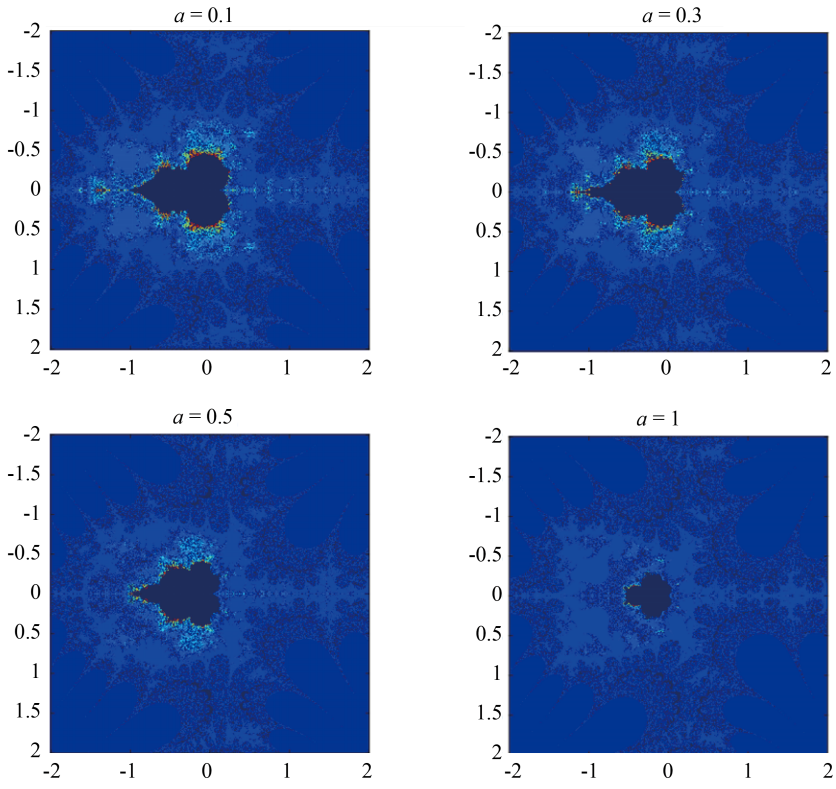


Figure 10. Effect of a on Mandelbrot set

Table 9. Parameters used to generate the Mandelbrot set for various values of a

S.N.	s	t	σ	a	n
1	0.01	0.09	0.05	0.30	2
2	0.01	0.09	0.05	0.50	2
3	0.01	0.09	0.05	0.90	2
4	0.01	0.09	0.05	1.00	2

6. Comparison of iterative methods

Example 1 Consider a Banach space $\mathscr{P} = \mathbb{R}$. We define the non-linear function $S(\zeta) = \frac{1}{2}\zeta + 1$, that has a unique fixed point. We take the Initial values: $u_0 = 1$, $\phi = 0.75$, $\psi = 0.8$ and s = 1. We compare the performance of different iterative schemes for approximating the fixed point. See Figure 11 and Table 10 for details.

All these methods converge to the fixed point $x^* = 2$, but the convergence rate may vary. The new algorithm typically converges faster due to a more balanced use of $\mathscr{P}$.

Table 10. Comparison of iterative values for different methods

Fun_n	Mann	Noor	Picard mann	Fibonacci	Extended fibonacci
0	1	1	1	1	1
1	1.375	1.5981	1.6875	1.75	1.9844
2	1.6094	1.8385	1.9023	1.9375	1.9998
3	1.7559	1.9351	1.9695	1.9844	2
4	1.8474	1.9739	1.9905	1.9961	2
5	1.9046	1.9895	1.997	1.999	2
6	1.9404	1.9958	1.9991	1.9998	2
7	1.9627	1.9983	1.9997	1.9999	2
8	1.9767	1.9993	1.9999	2	2
9	1.9854	1.9997	2	2	2
10	1.9909	1.9999	2	2	2
11	1.9943	2	2	2	2
12	1.9964	2	2	2	2
13	1.9978	2	2	2	2
14	1.9986	2	2	2	2
15	1.9991	2	2	2	2
16	1.9995	2	2	2	2
17	1.9997	2	2	2	2
18	1.9998	2	2	2	2
19	1.9999	2	2	2	2
20	1.9999	2	2	2	2
21	1.9999	2	2	2	2
22	2	2	2	2	2
23	2	2	2	2	2

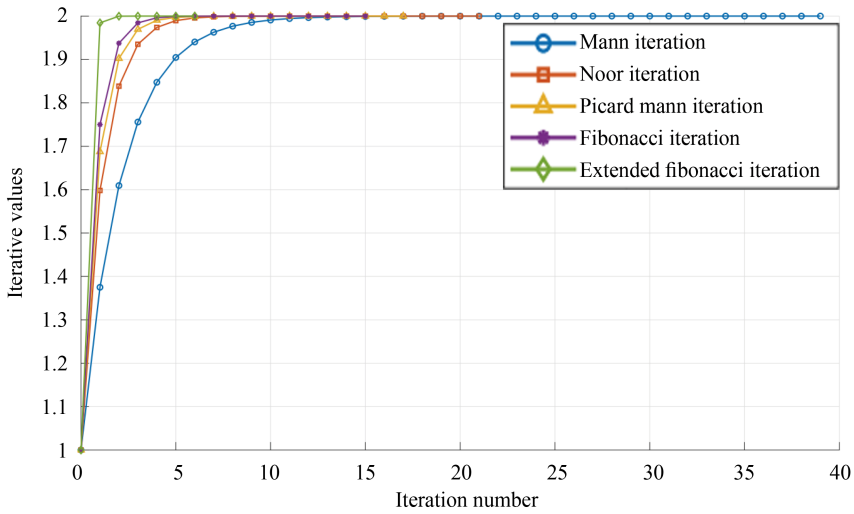


Figure 11. Convergence of the different iterative methods

7. Conclusion

An extended Fibonacci-Mann iteration is utilized in this research project in order to produce and evaluate Julia and Mandelbrot sets that were derived from complex sine functions. When different parameters were changed, a large number of fractal formations that were unexpected and intriguing were revealed. This method helped us clearly see and understand the rich and complex designs within these fractals, and the convergence of the iteration ensured the reliability of the generated results.

Authors contribution

Conceptualization, Z.U.N. and T.K.; methodology, U.I.; software, Z.U.N and M.A.; validation, U.I. and I.-L.P.; formal analysis, I.-L.P. and M.A.; investigation, Z.U.N. and M.A.; resources, T.K.; data curation, U.I.; writing-original draft preparation, Z.U.N.; writing-review and editing, U.I.; visualization, I.-L.P. and M.A.; supervision, T.K. and I.-L.P.; project administration, U.I. and M.A.; funding acquisition, I.-L.P. All authors have read and agreed to the published version of the manuscript.

Availability of data and material

Data sharing does not apply to this article as no data sets were generated or analyzed during the current study.

Acknowledgment

The authors extend their gratitude to the Deanship of Graduate Studies and Scientific Research of the Islamic University of Madinah for the support provided to the PostPublication Program 4.

Conflict of interest

The authors declare that they have no competing interests.

References

[1] Mandelbrot BB. *The Fractal Geometry of Nature*. United States: WH Freeman and Co.; 1982.

[2] Falconer K. *Fractal Geometry: Mathematical Foundations and Applications*. Hoboken: John Wiley and Sons; 2013.

[3] Devaney RL. *A First Course in Chaotic Dynamical Systems: Theory and Experiment*. Florida: CRC Press; 1992.

[4] Rani M, Kumar V. Superior julia set. *Research in Mathematical Education*. 2004; 8(4): 261-277.

[5] Chauhan YS, Rana R, Negi A. New tricorn and multicorns of Ishikawa iterates. *International Journal of Computer Applications*. 2010; 7(13): 25-33.

[6] Kang SM, Rafiq A, Latif A, Shahid AA, Ali F. Fractals through modified iteration scheme. *Filomat*. 2016; 30(11): 3033-3046.

[7] Zou C, Shahid AA, Tassaddiq A, Khan A, Ahmad M. Mandelbrot sets and Julia sets in Picard-Mann orbit. *IEEE Access*. 2020; 8: 64411-64421.

[8] Rani M, Chugh R. Julia sets and Mandelbrot sets in Noor orbit. *Applied Mathematics and Computation*. 2014; 228: 615-631.

[9] Li D, Shahid AA, Tassaddiq A, Khan A, Guo X, Ahmad M. CR iteration in generation of antifractals with *s*-convexity. *IEEE Access*. 2020; 8: 61621-61630.

[10] Cho SY, Shahid AA, Nazeer W, Kang SM. Fixed point results for fractal generation in Noor orbit and *s*-convexity. *SpringerPlus*. 2016; 5(1): 1843.

[11] Rawat S, Prajapati DJ, Tomar A, Dimri RC. Application of fixed point iterations in generation of fractals for higher-order complex polynomial. In: *Banach Contraction Principle: A Centurial Journey*. Singapore: Springer Nature Singapore; 2025. p.137-161.

[12] Nawaz B, Gdawiec K, Ullah K, Aphane M. A study of Mandelbrot and Julia Sets via Picard-Thakur iteration with s-convexity. *PLoS One*. 2025; 20(3): e0315271.

[13] Thompson JMT. Chaos, fractals and their applications. *International Journal of Bifurcation and Chaos*. 2016; 26(13): 1630035.

[14] Le BB. Chaotic dynamics and fractal geometry in ring lattice systems of nonchaotic Rulkov neurons. *Fractal and Fractional*. 2025; 9(9): 584.

[15] Lee JS, Chang KS. Applications of chaos and fractals in process systems engineering. *Journal of Process Control*. 1996; 6(2-3): 71-87.

[16] Djeacoumar A, Mujkanovic F, Seidel HP, Leimkühler T. Learning image fractals using chaotic differentiable point splatting. *arXiv:2502.17230*. 2025. Available from: https://doi.org/10.48550/arXiv.2502.17230.

[17] Falconer K. *Fractal Geometry: Mathematical Foundations and Applications*. United States: John Wiley & Sons; 2003.

[18] Schroeder M. *Fractals, Chaos, Power Laws: Minutes from an Infinite Paradise*. Mineola: Dover Publications; 1991.

[19] Wang D, Zhang Y, Lou W, Zang W. Fractal viewpoint in supply chain price competition. *Chaos, Solitons & Fractals*. 2023; 176: 114139.

[20] Antal S, Tomar A, Prajapati DJ, Sajid M. Variants of Julia and Mandelbrot sets as fractals via Jungck-Ishikawa fixed point iteration system with *s*-convexity. *AIMS Mathematics*. 2022; 7(6): 10939-10957.

[21] Gdawiec K, Shahid AA. Fixed point results for the complex fractal generation in the S-iteration orbit with *s*-convexity. *Open Journal of Mathematical Science (OMS)*. 2018; 2(1): 56-72.

[22] Özgür N, Antal S, Tomar A. Julia and mandelbrot sets of transcendental function via fibonacci-mann iteration. *Journal of Function Spaces*. 2022; 2022(1): 2592573.

[23] Antal S, Özgür N, Tomar A, Gdawiec K. Fractal generation via generalized Fibonacci-Mann iteration with *s*-convexity. *Indian Journal of Pure and Applied Mathematics*. 2024; 56: 1593-1607.

[24] Julia G. Dissertation on the iteration of rational functions [Mémoire sur l'itération des fonctions rationnelles]. *Journal of Pure and Applied Mathematics [Journal de Mathématiques Pures et Appliquées]*. 1918; 1: 47-245.

[25] Rossi M, Buratti G. Fractal patterns. Forms of nature for project sustainability. *Disegnarecon*. 2021; 14(26): 1-17.

[26] Gdawiec K, Kotarski W, Lisowska A. On the robust Newton's method with the Mann iteration and the artistic patterns from its dynamics. *Nonlinear Dynamics*. 2021; 104(1): 297-331.

[27] Kwun YC, Shahid AA, Nazeer W, Abbas M, Kang SM. Fractal generation via CR iteration scheme with *s*-convexity. *IEEE Access*. 2019; 7: 69986-69997.

[28] Noor MA, Noor KI, Bnouhachem A. Some new iterative methods for solving variational inequalities. *Canadian Journal of Applied Mathematics*. 2020; 2(2): 1-7.

[29] Shahid AA, Nazeer W, Gdawiec K. The Picard-Mann iteration with *s*-convexity in the generation of Mandelbrot and Julia sets. *Monthly Journals for Mathematics [Monatshefte für Mathematik]*. 2021; 195(4): 565-584.